Soft Matter

ARTICLE TYPE

Cite this: DOI: 00.0000/xxxxxxxxxx

Formation of Colloidal Chains and Driven Clusters with Optical Binding: Supplementary Material

Dominique Davenport and Dustin Kleckner

1 Optical scattering, gradient, and binding forces

The analysis in the manuscript was guided by comparing two types of scattering bodies, Polystyrene (PS) and Silica (SiO_2) particles, denoted as HIP and LIP. Initial calculations were done comparing the relative strengths of three optical forces: the scattering force, gradient force, and binding force.

The scattering force is a first-order optical force which arises from the back-reflection of incident photons[?]. The scattering force is non-conservative and is dependent on the direction of light propagation. We determine the strength of the force through simulating a single particle in single plane wave.

The gradient force is a first-order optical force due to the induced dipole moments generated in the scattering object by the incident light[29]. The force is completely conservative and is highly depended on the gradients in the electric field. We determine the strength of the force through simulating a single particle in a standing wave generated by two counter-propagating plane waves. The two counter-propagating waves negate scattering forces, the standing wave pattern generates gradients in the optical field which apply gradient forces onto the single object.

The optical binding force is a second-order optical force due to the modification of an incident field on an object by the scattered fields of other objects[11]. Optical binding is a combination of conservative and non-conservative forces. We simulate the force by placing two objects separated in cross-polarized counter-propagating plane waves. The counter-propagation negates the first-order scattering forces while cross-polarizing removes the standing wave suppressing the first-order gradient force. Remaining forces must be due to optical binding effects.

At the size range of interest we find that PS particles have relatively stronger scattering forces while LIPs have relatively stronger gradient forces. The conclusion made is that HIPs are stronger scatterers.

2 Numerical Simulations

The numerical simulations were achieved using a Coupled Dipole Method (CDM) based scattering code[27,28]. In each case, we ensure 10 dipoles per wavelength is used. We use an iterative solver in which the number of iterations are set until the root mean square of the dipole moments converge to $< 1\%$.

The 2-dimensional maps were generated by running a stand-alone simulation at each particle displacement. A single particle was fixed at an origin while a second particle was moved along a 2-dimensional space on the plane in the immediate vicinity of the fixed particle.

3 Force map generation

The force maps were generated using CDM based simulation. By placing two particles in a cross-polarized counter-propagating field, we calculate the radiation forces placed on each particle. Filling out the 2-dimensional space is done by fixing one object at an origin and repeating the simulation for various displacements.

4 Correlating volume mean squared difference (VMSD) with mean squared displacement (MSD)

3-Dimensional videos were taken of particles undergoing Brownian motion. 19 individual particles located in a single volume were averaged to generate a reference particle. We used the reference particle to simulate particle motion by shifting it a known amount in a generated noisy background. The results of the simulated displacements along different axes are provided in **Fig. 1**. We can correlate the size of the simulated step to the value of taking the sum squared volume difference (VSD) of the array before and after the step. We found that larger displacements correspond to a larger VSD in general. One limitation is that the motion in the z-direction is underrepresented compared to motion in the x-y plane due to the inherent asymmetry of the particles imaging profile along the z-axis. This limitation does not allow us to place an absolute estimate of how

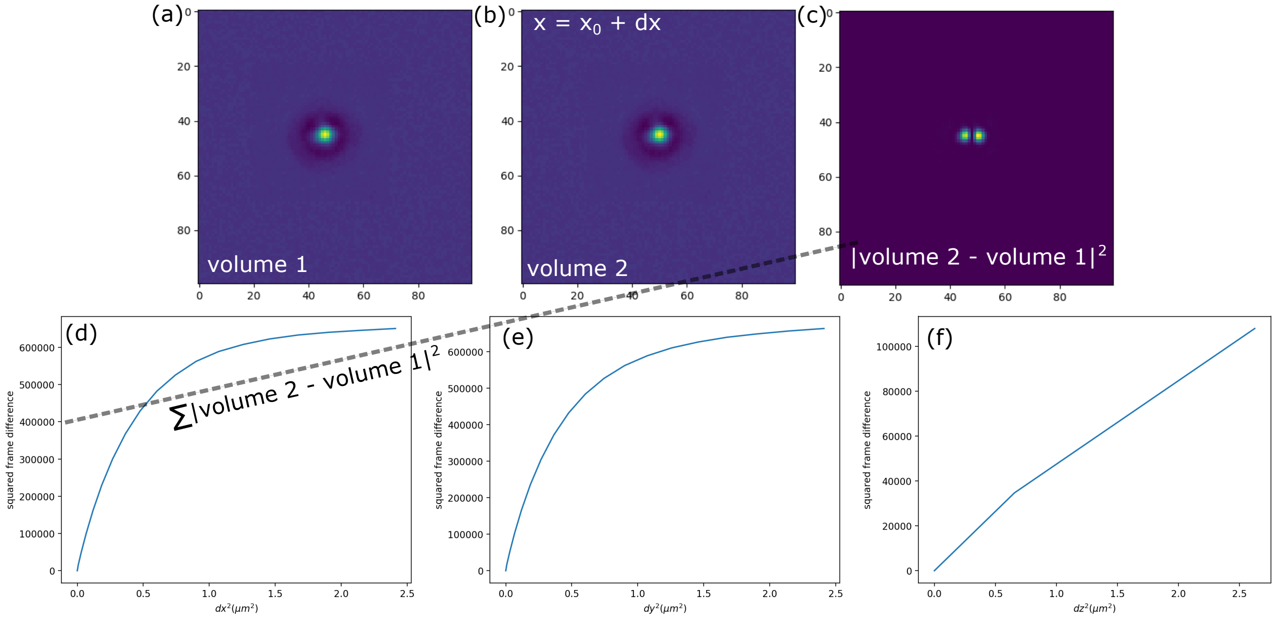

Fig. 1 A simulated PS particle displaced along the x, y, and z axis plotted against a corresponding squared volume difference.

fast the objects are moving in physical units; however we can still measure the relative motion under the assumption that the motion in the compared systems share similar axial preferences. Observations of the data support this assumption. The second limitation is that the VSD value is capped at displacements that are slightly larger than the particle diameter. At the volume rate of 10 volumes/s, particles undergoing Brownian motion are moving slow enough; however we have observed that particles undergoing optical binding forces can be propelled much faster. One way to alleviate the limitation is to record at a higher volume rate; however, it is currently unfeasible to cover the full range of possible particle speeds. This limitation is also present in traditional tracking methods.

Although the motion of the fastest particles are underrepresented in the VSD values, the VMSD method still allows a maximum value to be assigned. Traditional tracking methods would not be able to assign a velocity value at all. We also note that underrepresenting the motion of the faster moving particles only acts to underrepresent the strength of the findings.

The VMSD at any given time is determined by subtracting two subsequent volumes from each other, removing the contribution from the background, and dividing by the total number of particles in the frame:

$$\Delta(t) = \frac{1}{N_p(t)}\left[\sum_{i,j,k}^{volume}(p_{i,j,k,t} - p_{i,j,k,t-dt})^2 - \Delta_0\right] \quad (1)$$

The background contribution, Δ_0, is determined in each video by monitoring the squared difference of sections that have zero particles. We find a non-zero constant value which can be subtracted to remove contributions that are due to noise. The number of particles, N_p, is estimated by the following:

$$N_p = c_0 \sum_{i,j,k}^{volume} |p_{i,j,k,t} - b_{i,j,k}| + c_1 \quad (2)$$

Where $b_{i,j,k}$ is belongs to a volume representing the sample devoid of particles. c_0 and c_1 are fitting parameters determined by linearly fitting the number of particles found by traditional tracking methods to $\sum_{i,j,k}^{volume} |p_{i,j,k,t} - b_{i,j,k}|$ for a system of particles undergoing Brownian motion. Some results in **Fig. 2**. For the HIPs, we show that for diffusive particles and particles interacting in a weak field, there is a clear correlation between the VMSD and the true MSD (**Fig. 2**). For the LIPs, we also find correlation between the VMSD and true MSD for the diffusive particles; however in a weak field, the correlation is reduced. We found that in a weak field, the Lower-index particles tended to pack into tight formations which effected the individual tracking capabilities. Thus we utilize the purely diffusive correlation to justify the use of VMSD in a difficult tracking atmosphere.

We represent the motion in terms of the VMSD values relative to the Brownian Motion case. Doing so allows us to compare the HIP and LIP systems in how their motion changes relative to diffusive motion.

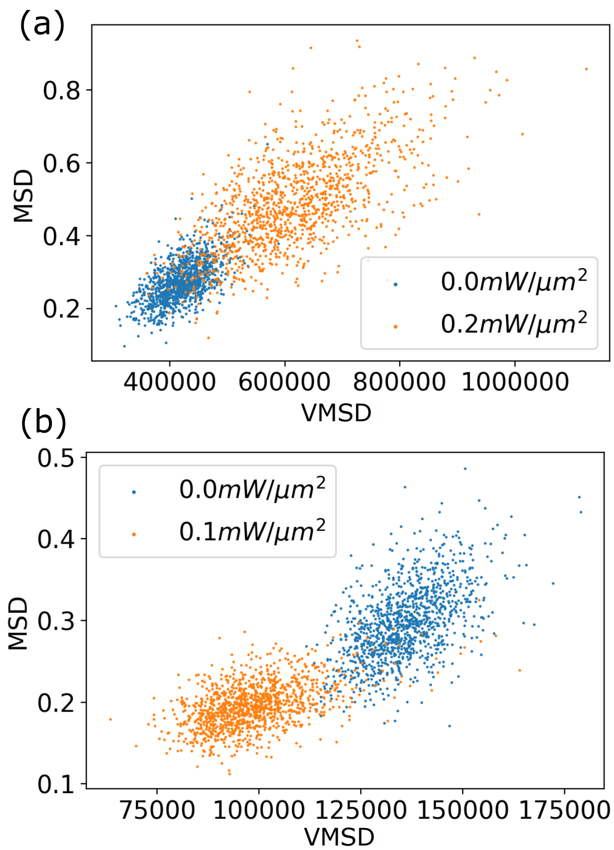

Fig. 2 VMSD values compared to 2-dimensional mean squared displacement (MSD) in the xy-plane for (a) HIP (PS) and (b) LIP (SiO_2) particles.

5 Electronic Supplementary Information

All movies are 2 mins played in real-time.

5.1 Movie S1

HIP (Polystyrene) particles in cross polarized counter-propagating beam (peak power density - 1.5 mW/μm^2).

5.2 Movie S2

LIP (SiO_2) particles in cross polarized counter-propagating beam (peak power density - 1.5 mW/μm^2).

5.3 Movie S2

HIP (Polystyrene) particles in standing wave (peak power density - 1.5 mW/μm^2).

Notes and references

1 G. M. Whitesides and B. Grzybowski, *Science*, 2002, **295**, 2418–2421.

2 B. A. Grzybowski, C. E. Wilmer, J. Kim, K. P. Browne and K. J. M. Bishop, *Soft Matter*, 2009, **5**, 1110.

3 F. Ginot, I. Theurkauff, F. Detcheverry, C. Ybert and C. Cottin-Bizonne, *Nature Communications*, 2018, **9**, 696.

4 A. Wang, W. Shi, J. Huang and Y. Yan, *Soft Matter*, 2015, **12**, 337–357.

5 J. R. Howse, R. A. L. Jones, A. J. Ryan, T. Gough, R. Vafabakhsh and R. Golestanian, *Physical Review Letters*, 2007, **99**, 048102.

6 B. A. Grzybowski, H. A. Stone and G. M. Whitesides, *Nature*, 2000, **405**, 1033–1036.

7 B. A. Grzybowski, H. A. Stone and G. M. Whitesides, *Proceedings of the National Academy of Sciences*, 2002, **99**, 4147–4151.

8 G. Kokot, G. V. Kolmakov, I. S. Aranson and A. Snezhko, *Scientific Reports*, 2017, **7**, 14726.

9 P. Tierno, R. Golestanian, I. Pagonabarraga and F. Sagués, *Physical Review Letters*, 2008, **101**, 218304.

10 A. Snezhko and I. S. Aranson, *Nature Materials*, 2011, **10**, 698–703.

11 M. M. Burns, J.-M. Fournier and J. A. Golovchenko, *Physical Review Letters*, 1989, **63**, 1233–1236.

12 T. Thirunamachandran, *Molecular Physics*, 1980, **40**, 393–399.

13 J. Bai, Z.-S. Wu and C.-X. Ge, 2018 12th International Symposium on Antennas, Propagation and EM Theory (ISAPE), 2018, pp. 1–3.

14 X. Li, Y. Liu, Z. Lin, J. Ng and C. T. Chan, *Nature Communications*, 2021, **12**, 6597.

15 F. Dapasse and J. M. Vigoureux, *Journal of Physics D: Applied Physics*, 1994, **27**, 914–919.

16 S. K. Mohanty, J. T. Andrews and P. K. Gupta, *Optics Express*, 2004, **12**, 2746–2753.

17 S. A. Tatarkova, A. E. Carruthers and K. Dholakia, *Physical Review Letters*, 2002, **89**, 283901.

18 J. Ng, Z. F. Lin, C. T. Chan and P. Sheng, *Physical Review B*, 2005, **72**, 085130.

19 N. K. Metzger, K. Dholakia and E. M. Wright, *Physical Review Letters*, 2006, **96**, 068102.

20 V. Karásek, T. Čižmár, O. Brzobohatý, P. Zemánek, V. Garcés-Chávez and K. Dholakia, *Physical Review Letters*, 2008, **101**, 143601.

21 K. Dholakia and P. Zemánek, *Reviews of Modern Physics*, 2010, **82**, 1767–1791.

22 J. Rodríguez, L. C. Dávila Romero and D. L. Andrews, *Physical Review A*, 2008, **78**, 043805.

23 K. A. Forbes, D. S. Bradshaw and D. L. Andrews, *Nanophotonics*, 2020, **9**, 1–17.

24 F. Nan, F. Han, N. F. Scherer and Z. Yan, *Advanced Materials*, 2018, **30**, 1803238.

25 O. Brzobohatý, L. Chvátal, M. Šiler and P. Zemánek,

Optics Express, 2020, **28**, 37700.

26 Z. Yan, S. K. Gray and N. F. Scherer, *Nature Communications*, 2014, **5**, 3751.

27 B. T. Draine and P. J. Flatau, *JOSA A*, 1994, **11**, 1491–1499.

28 A. G. Hoekstra, M. Frijlink, L. B. F. M. Waters and P. M. A. Sloot, *JOSA A*, 2001, **18**, 1944–1953.

29 A. Ashkin, J. M. Dziedzic, J. E. Bjorkholm and S. Chu, *Optics Letters*, 1986, **11**, 288–290.

30 M.-T. Wei, J. Ng, C. T. Chan and H. D. Ou-Yang, *Scientific Reports*, 2016, **6**, 38883.

31 V. Karásek, K. Dholakia and P. Zemánek, *Applied Physics B*, 2006, **84**, 149–156.

32 V. Karásek, O. Brzobohatý and P. Zemánek, *Journal of Optics A: Pure and Applied Optics*, 2009, **11**, 034009.

33 W. Singer, M. Frick, S. Bernet and M. Ritsch-Marte, *JOSA B*, 2003, **20**, 1568–1574.

34 X. Zhang, J. Qiu, J. Qiu, J. Qiu, X. Li, X. Li, J. Zhao, J. Zhao, L. Liu and L. Liu, *Applied Optics*, 2020, **59**, 2337–2344.

35 G. M. Hale and M. R. Querry, *Applied Optics*, 1973, **12**, 555–563.

36 I. H. Malitson, *JOSA*, 1965, **55**, 1205–1209.

37 J. C. Crocker and D. G. Grier, *Journal of Colloid and Interface Science*, 1996, **179**, 298–310.

38 D. Allan, T. Caswell, N. Keim and C. van der Wel, *trackpy: Trackpy v0.3.0*, 2015, `https://zenodo.org/record/34028`.